Extremophiles (2011) 15:67–76
DOI 10.1007/s00792-010-0338-z

ORIGINAL PAPER

Single-stranded DNA binding activity of XPBI, but not XPBII, from *Sulfolobus tokodaii* causes double-stranded DNA melting

Xiaoqing Ma · Ye Hong · Wenyuan Han · Duohong Sheng · Jinfeng Ni · Guihua Hou · Yulong Shen

Received: 19 July 2010 / Accepted: 12 November 2010 / Published online: 5 December 2010
© Springer 2010

Abstract XPB helicase is the largest subunit of transcription factor IIH (TFIIH), a ten-subunit protein complex essential for transcription initiation and nucleotide excision repair (NER) in Eukarya. Two XPB homologues (XPBI and XPBII) are present in the genome of most crenarchaeota, one of the two major phyla of archaea; however, the biochemical properties have not been fully characterized and their cellular roles have not been clearly defined. Here, we report that XPBI from the hyperthermophilic crenarchaeon *Sulfolobus tokodaii* (StoXPBI) is able to destabilize double-stranded DNA (dsDNA) helix independent of ATP (designated as dsDNA melting activity). This activity is inhibited by single-stranded DNA (ssDNA) and relies on the unique N-terminal domain of StoXPBI, which is also likely responsible for the intrinsic strong ssDNA binding activity of StoXPBI as revealed by deletion analysis. We demonstrate that the ATPase activity of StoXPBII is remarkably stimulated by StoBax1, a nuclease partner of StoXPBII. The role of the unique dsDNA melting activity of XPBI in NER in archaea was discussed.

Communicated by T. Matsunaga.

Electronic supplementary material The online version of this article (doi:10.1007/s00792-010-0338-z) contains supplementary material, which is available to authorized users.

X. Ma · Y. Hong · W. Han · D. Sheng · J. Ni · Y. Shen (✉)
State Key Laboratory of Microbial Technology,
Shandong University, 27 Shanda Nan Rd.,
Jinan 250100, People's Republic of China
e-mail: yulgshen@sdu.edu.cn

G. Hou
School of Medicine, Shandong University,
Jinan 250012, People's Republic of China

Keywords Archaea · Nucleotide excision repair · *Sulfolobus tokodaii* · XPB · Bax1

Introduction

DNA helicase is a large family of enzymes that unwind double-stranded DNA (dsDNA) coupling with the energy of ATP hydrolysis. XPB helicase is the largest subunit of transcription factor IIH (TFIIH), a ten-subunit protein complex essential for transcription initiation and nucleotide excision repair (NER) in eukarya (Schaeffer et al. 1993; Drapkin et al. 1994; Giglia-Mari et al. 2004). It belongs to superfamily II helicase and unwinds dsDNA in 3′ to 5′ direction depending on ATP hydrolysis (Guzder et al. 1994). *xpb* was originally identified as a primary responsible gene for NER defects in XP-B (xeroderma pigmentosum, group B) patients (Thompson et al. 1987). Mutations in XPB have also been associated with two genetically heterogeneous human syndromes, Cockayne's syndrome (CS), and trichothiodystrophy (TTD) (Vermeulen et al. 1994; Hwang et al. 1996).

The cellular functions of XPB in eukarya have not been fully understood. In vitro reconstitution studies on TFIIH suggest that XPB may not be a conventional helicase but an ATPase in NER and transcription (Jawhari et al. 2002; Lin et al. 2005; Coin et al. 2007; Oksenych et al. 2009); however, the functional details of the ATPase need to be clarified. In addition, although it has been found that the activity of XPB is modulated by its interactions with other subunits of TFIIH (Jawhari et al. 2002), and XPB seems to play an important role in the recruitment and redistribution of XPG, XPA, and XPF (Coin et al. 2004; Oh et al. 2007), the details of the protein–protein interactions remain unclear.

Archaeal and eukaryotic information processing apparatus are strikingly similar (Ishino et al. 2006) and they share NER orthologues including nucleases XPF and XPG, and helicases XPB and XPD (reviewed by White 2003). Studies on the structures and biochemistry of individual proteins involved in NER of archaea have made great progress in recent years. The in vitro activities of the 5′-3′ helicase XPD and the nuclease XPF have been reported, indicating that they are similar to those of their eukaryotic counterparts in general (Roberts and White 2005a, b; Rudolf et al. 2006). And the structure of archaeal XPD has given insights into the consequences of XPD mutations on human diseases (Fan et al. 2008; Liu et al. 2008; reviewed by Lehmann 2008).

Most archaea have one or two XPB homologues which share 23–28% identities with human XPB (Richards et al. 2008; Biswas et al. 2009). The structure of XPB and the in vitro activities of XPB and XPB/Bax1 (the nuclease partner of XPB or XPBII) have been reported (Fan et al. 2006; Richards et al. 2008; Roth et al. 2009; Rouillon and White 2010). However, the mutual interactions between XPB and Bax1 are still mysterious, and Bax1s from *S. solfataricus* and *T. acidophilum* exhibit nuclease activities with unexpected difference (Rouillon and White 2010). In addition, the function of XPBI in crenarchaeota has not been defined.

In this paper, we show that XPBI from the hyperthermophilic *Sulfolobus* has a novel helix-destabilization (dsDNA melting) activity which is independent of ATP and caused by its strong ssDNA binding ability. The unique N-terminal domain of XPBI is essential for its ssDNA binding and dsDNA melting activity. In addition, we find that Bax1 promotes the ATPase activity of XPBII in the presence of dsDNA.

Materials and methods

Gene cloning and plasmid construction

The gene encoding StoXPBI (ST1287), StoXPBII (ST1613), StoBax1 (ST1614), and StoSSB (ST0503) were amplified from genomic DNA of *S. tokodaii* strain 7 using *Pfu* polymerase (Bioteke, China). The NdeI/XhoI restriction sites were introduced into the gene fragment of StoXPBI using 5′-GCCGGCATATGCTCTTGAAGACTTTTTATACACA GCAAT-3′ (upstream primer) and 5′-GGCCGCTCGAG TTATACCAAATCTTCTTCTGAAGAGGAA-3′ (downstream primer). The NdeI/SalI restriction sites were introduced into the gene fragment of StoXPBII using 5′-CGG CGGCATATGGTATACTTAAGATACTTTAAAGGG-3′ (upstream primer), and 5′-TTTGCGGTCGACTCATTC TCTCCTTCTCCTACTTA-3′ (downstream primer), and gene fragment of StoBax1 using 5′-CGACTCATATGT TACCGTGGGAATTAGCAAG-3′ (upstream primer) and 5′-CGGCGGGTCGACTTAATTTACTTTTTTGTCC-3′ (downstream primer). The NdeI/BamHI restriction sites were introduced into the gene fragment of StoSSB using 5′-GGCATATGAGTCGAATGGGAGAAGAGAA-3′ (upstream primer) and 5′-CCGGATCCTCAGAATTCTTC CTCACCACTCTCT-3′ (downstream primer). The PCR products were digested with the corresponding restriction enzymes, and the genes were cloned into the NdeI/SalI sites of a modified pET15b (the NcoI site of original pET15b was changed to NdeI site and a SalI site was added in the multiple cloning site) for the expression of native XPBs, the NdeI/SalI sites and the NdeI/BamHI sites of pET15b for the expression of His-tagged Bax1 and SSB. The deletion mutants StoXPBI(112–543) and StoXPBI(1–111) were constructed by PCR amplification of the gene fragments using specifically designed primers and the plasmid DNA as the template, digestion with NdeI and XhoI, and cloning into the NdeI/SalI sites of the modified pET15b. The site-directed mutant StoXPBI(K186A) was constructed by overlap PCR amplification using the corresponding primers, digestion with NdeI and XhoI, and cloning into the NdeI/SalI sites of the modified pET15b. The nucleotide sequences of the inserted genes were confirmed by sequencing (Invitrogen, Shanghai, China).

Expression and purification of recombinant proteins

The constructed plasmid pET15b/StoXPBI was transformed into *E. coli* BL21-CodonPlus (DE3)-RIL. The transformed cells were then cultured in Luria–Bertani (LB) broth containing 100 mg/L ampicillin and 34 mg/L chloramphenicol at 37°C. When the OD_{600} reached 0.4, the expression was induced by the addition of 0.5 mM IPTG. After growth for further 4 h at 37°C, the cells were harvested by centrifugation and disrupted by sonication in buffer A (50 mM Tris–HCl, pH 8.0 and 100 mM NaCl). The disrupted cells were heated at 75°C for 30 min. The heat-resistant supernatant was precipitated with 100% saturated ammonium sulfate. The precipitated protein was re-suspended in buffer A and dialyzed against buffer A to remove the ammonium sulfate. After dialysis and filtration, the sample was loaded onto a 5 ml HiTrap Q column pre-equilibrated with buffer B (50 mM Tris–HCl, pH 8.8, and 100 mM NaCl). The fractions eluted at 250–320 mM NaCl were collected and loaded onto Sephacryl S-200 gel filtration column for further purification. StoXPBII and the two deleted mutants of StoXPBI were expressed and purified in the same way as for XPBI.

The His-tagged StoBax1 and StoSSB proteins were expressed as described above for XPB proteins. After sonication of the cells and heat treatment of the disrupted cells, ammonium sulfate precipitation was performed.

The precipitated protein was re-suspended in buffer A and loaded onto a 1 ml nickel nitrilotriacetic acid-agarose column. The column was washed with ten column volumes of buffer A containing 60 mM imidazole and eluted with three column volumes of elution buffer containing 150 mM imidazole. The eluted fractions were pooled, concentrated, and separated on a Sephacryl S-200 gel filtration column. Protein concentrations were measured by the Bradford method.

Preparation of DNA substrates

Oligonucleotides (Table 1) were labeled at the 5′ ends using T4 polynucleotide kinase and ATP-γ-^{32}P. The final concentration of the oligonucleotide in the labeling mixture was 1,000 nM. The annealing reaction was performed in a 50 μl mixture which contained 40 mM Tris–acetate (pH 7.8), 0.5 mM magnesium acetate, 200 nM unlabeled oligonucleotides, and 100 nM labeled oligonucleotides. The mixture was boiled at 95°C for 5 min and gradually cooled down to room temperature. The annealed substrates were purified by gel electrophoresis (6% polyacrylamide) in TBE buffer (45 mM Tris–borate, 1 mM EDTA). The bands corresponding to the substrates were excised and eluted from the gel by diffusion at room temperature for 18–36 h into a buffer (25 mM Tris–HCl, pH 8.0 containing 50 mM NaCl).

Pull-down assay

The mixture of His-tagged StoBax1 (50 μg) and equal amount of native StoXPBII were incubated in buffer A on ice for 30 min. The mixture was then blended with 40 μl of nickel nitrilotriacetic acid-agarose slurry pre-equilibrated with buffer A. The agarose beads were collected by centrifugation at 3,000×*g* for 3 min and washed five times at room temperature in 1 ml of wash buffer (50 mM Tris–HCl, pH 8.0, 100 mM NaCl, and 60 mM imidazole). Next, 20 μl of loading buffer (250 mM Tris–HCl, 0.5% SDS, 50% glycerol, 0.5% bromophenol blue, and 500 mM DTT) was added to the samples. The samples were then boiled for 10 min and loaded on a 12% SDS polyacrylamide gel. After electrophoresis, the gel was stained with Coomassie bright blue. StoXPBII and His-tagged StoBax1 were also loaded separately as the controls.

DNA binding assay

DNA binding assay was carried out in a 20 μl mixture containing 25 mM Tris–HCl (pH 8.0), 5 mM magnesium chloride, 1 mM DTT, 25 mM NaCl, 2 nM DNA substrate, 12% glycerol, and gradient concentrations of enzyme (0–1 μM for ssDNA and 0–8 μM for dsDNA). The mixture was incubated at 37°C for 30 min and then loaded on a 6% polyacrylamide gel in TBE buffer. Samples were electrophoresed at 120 V for 60–90 min. The K_d values were calculated as the concentration of protein that retarded 50% of the labeled DNA.

ATPase assay

ATPase activity was analyzed in a 20 μl mixture containing 25 mM Tris–HCl (pH 8.0), 25 mM NaCl, 5 mM magnesium chloride, 0.5 mM DTT, 1 mM ATP, 0.2 μCi labeled [γ-^{32}P] ATP, 500 nM of the enzymes, and 10 nM of supercoiled dsDNA or virion ssDNA. The mixture was incubated at 50°C for indicated time. The reaction was terminated by the addition of EDTA to a final concentration of 50 mM. Two-microliter aliquots were spotted onto polyethyleneimine-cellulose plates (Merck, Germany). ATP and released Pi were then separated chromatographically in 1 M formic acid and 0.5 M LiCl. The ATPase assay of StoXPBII in the presence of StoBax1 was conducted with 100 nM StoXPBII, indicated concentrations of StoBax1 and 3 nM supercoiled double-stranded plasmid DNA. The ATPase analysis of StoXPBI in the presence of StoBax1 was performed with 500 nM StoXPBI, indicated concentrations of StoBax1, and 10 nM supercoiled

Table 1 The substrates used in this study

Name	Structure	Oligonucleotide sequences
S1		E: *5′-CAAGCTTGCATGCCTGCAGGTCGACTCTAGAGGA-3′ (34 mer)
		F: 5′-TCCTCTAGAGTCGACCTGCAGGCATGCAAGCTTG-3′ (34 mer)
S2		E: as in S1
		B: 5′-TCCTCTAGAGTCGACCTGCAGGCATGCAAGCTTGGCACTGGC CGTCCTTTTACAACGTCGTGACTGGGAAAACCCTGGCGTTAC-3′ (84 mer)
A		A: 5′-GTAACGCCAGGGTTTTCCCAGTCACGACGTTGTA-3′ (34 mer)

✷ indicates the site where the substrates were labeled

double-stranded plasmid DNA. The reaction mixture was incubated at 50°C for 12 min.

DNA helicase and melting activity assays

Standard helicase activity assay was performed in a 20 µl mixture containing 25 mM Tris–HCl (pH 8.0), 25 mM NaCl, 5 mM magnesium chloride, 1 mM DTT, 1 nM DNA substrate, 1 mM ATP, and the indicated concentrations of the enzyme. The mixtures were incubated at 50°C for 20 min, and the reactions were stopped by the addition of 10 µl of stop buffer containing 20 mM protease K, 50 mM EDTA, 0.5% SDS, 25% glycerol, and 0.025% bromophenol blue. The mixtures were then loaded onto a 10% polyacrylamide gel and electrophoresed at 150 V for 60 min in TBE buffer. Standard melting activity was analyzed as for the helicase activity assay except that 1 mM ATP was omitted.

Data collection and quantification

All polyacrylamide gels and polyethyleneimine-cellulose plates were exposed to a phosphor imager (GE). The phosphor imager was scanned using the Storm840 scanner (GE). The images were analyzed using Image Quant 5.0 software (GE). All the results were based on at least triplicate measurements.

Results

Expression and purification of XPBI, XPBII, Bax1, and SSB from *S. tokodaii*

As in many other crenarchaeota, there are genes encoding XPBI, XPBII, and Bax1 homologues, respectively, in the genome of *S. tokodaii* (Richards et al. 2008). The proteins, StoXPBI (ST1287, 62 kDa), StoXPBII (ST1613, 51 kDa), and StoBax1 (ST1614, 57 kDa), have 37, 48, and 33% sequence identities with corresponding proteins from *A. fulgidus*, and 58, 64, and 48% with the corresponding proteins from *S. solfataricus*, respectively. XPBI and XPBII have similar catalytic cores of eukaryotic XPB which have 64% sequence identity, but lack the N- and C-terminal regulatory regions of XPB. Comparison of the amino acid sequences of XPB homologues reveals that StoXPBI is larger than StoXPBII due to its unique N-terminal 111 amino acid extension, whose function remains unknown (Fig. 1).

The genes encoding StoXPBI, StoXPBII, StoBax1, StoSSB and the mutants StoXPBI(1–111), StoXPBI (112–543), and StoXPBI(K186A) were cloned into pET15b or the modified pET15b and transformed into *E. coli* to express the proteins. Highly purified proteins were obtained by the procedures as described in the "Materials and methods". The purified proteins were analyzed by SDS-PAGE, and bands with expected sizes were present on the gel (Fig. 2).

DNA binding activity of StoXPBI, StoXPBII, and the mutants

Gel electrophoretic mobility shift assays (EMSAs) were conducted to assay the DNA binding ability of StoXPBI, StoXPBII, and deleted mutants of StoXPBI using 2 nM 34 mer ssDNA (E, Table 1) and blunt-ended 34 bp dsDNA (S1, Table 1) as the substrates and the results were summarized in Table 2. Both StoXPBI and StoXPBII bound ssDNA more tightly than dsDNA. StoXPBI had higher DNA binding activity than StoXPBII (Table 2). The results are consistent with the previous reports about XPBs from *S. solfataricus* (Richards et al. 2008). In order to understand the function of the N-terminal 111 amino acid domain, we examined effect of the N-terminal domain deletion on DNA binding. Interestingly, StoXPBI(112–543) exhibited remarkably reduced ssDNA binding affinity. The K_d value of StoXPBI (112–543) binding to ssDNA was close to that of StoXPBII (Table 2). While the K_d value of StoXPBI (112–543) to dsDNA decreased only slightly. At the same time, mutant StoXPBI(1–111) had notable ssDNA binding activity. These results suggest that the N-terminal

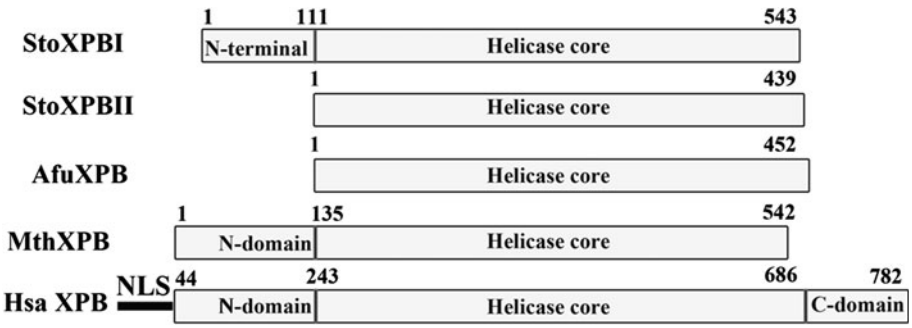

Fig. 1 Domain organization of XPB homologues from *S. tokodaii* (StoXPBI and StoXPBII), *Archaeoglobus fulgidus* (AfuXPB), *Mycobacterium tuberculosis* (MthXPB), and *Homo sapiens* (HsaXPB). The domain boundaries are indicated by *numbers*

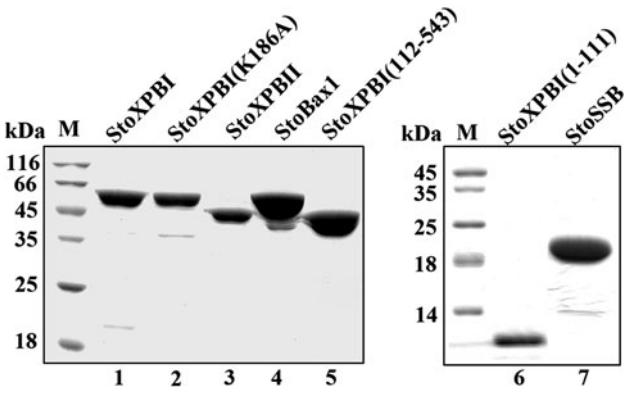

Fig. 2 SDS-PAGE analysis of the purified proteins: the expected molecular sizes of StoXPBI (lane *1*), StoXPBI(K186A) (lane *2*), StoXPBII (lane *3*), His-tagged StoBax1(lane *4*), StoXPBI(112–543) (lane *5*), StoXPBI(1–111) (lane *6*), StoSSB (lane *7*) are 62, 62, 51, 57, 49, 13 and 18 kDa, respectively. *M* molecular size markers

Table 2 Apparent K_d values exhibited by XPBI and XPBII

Substrates	K_d (μM)			
	StoXPBI	StoXPBII	StoXPBI (111–543)	StoXPBI (1–111)
34 nt ssDNA	0.04–0.06	0.16–0.3	0.1–0.2	~1
34 bp dsDNA	0.2–0.3	~6	~0.5	~8

domain of XPBI is important for strong ssDNA binding of StoXPBI.

DNA-dependent ATPase activities of StoXPBI and StoXPBII

The ATPase activities of both StoXPBI and StoXPBII were examined. In the absence of DNA, no apparent activity was observed for either enzyme (Fig. 3a). However, in the presence of a supercoiled double-stranded plasmid DNA or a single-stranded virion DNA of a modified plasmid pSK (Plank and Hsieh 2006) at the concentration of 10 nM (34 μM base pairs or nucleotides), ATPase activity was observed for both StoXPBI and StoXPBII (Fig. 3a). The ATPase activity of StoXPBI was stimulated more remarkably by single-stranded virion DNA than by plasmid DNA (Fig. 3a), while the ATPase of StoXPBII was more strongly stimulated by plasmid DNA (Fig. 3a). In addition, the average ATP hydrolysis rate of XPBII was evidently higher than that of XPBI which may indicate that the ATPase activities of XPBI and XPBII have different functions.

The ATPase activity of the deletion mutant StoXPBI(112–543) was also assayed. As shown in Fig. 3b, the mutant exhibited dsDNA and ssDNA-dependent ATPase activities which were similar to those of full-length StoXPBI. This result indicates that the N-terminal of XPBI plays no apparent role in the ATPase activity of XPBI.

StoXPBII specifically interacts with Bax1 in vitro

The interaction between StoXPBII and StoBax1 was examined using nickel agarose beads affinity pull-down assay. As shown in Fig. 4a, the N-terminal His-tagged StoBax1 was able to pull down StoXPBII that had no His-tag and was unable to bind the beads. We have also tested the possible interaction between StoXPBI and StoBax1 or StoXPBI(112–543) and StoBax1. However, no interaction was detected (data not shown). Thus, it is confirmed that XPBII and Bax1 from *S. tokodaii* can interact with each other specifically and form a stable complex in vitro.

StoBax1 stimulates the ATPase activity of StoXPBII

The effect of Bax1 on the ATPase activity of StoXPBII was assayed. As shown in Fig. 4b, c, StoBax1 remarkably stimulated the ATPase activity of StoXPBII in the presence of 3 nM supercoiled double-stranded plasmid DNA. With equal amount of StoBax1, the ATP hydrolysis of StoXPBII reached nearly three times as that without StoBax1. While under the same conditions, the ATPase activity of StoXPBI could not be promoted (Fig. 4d, e). Similar results were obtained by the malachite green assay (Supplementary Figure 2).

StoXPBI destabilizes dsDNA helix in the absence of ATP

Since StoXPBI and StoXPBII are supposed to be DNA helicases, we analyzed the unwinding activity of the two proteins using blunt-ended dsDNA and dsDNA with a 3′ extension as the substrates (S1 and S2, Table 1). We do have observed the ssDNA product when ATP was present in the reaction (Fig. 5). Unexpectedly, in the control in which ATP was not added, there was also ssDNA product (Fig. 5a, c). Although StoXPBI had DNA-dependent ATPase activity, addition of ATP did not lead to more ssDNA generated when a standard substrate of XPB was used (Fig. 5c, d). Consistently, Walk A mutant of XPBI (K186A) which lost its ATPase activity (data not shown) could also destabilize the dsDNA (Fig. 5b). This activity is in contrast to those of XPBs from eukarya and bacteria, which have helicase activity with 3′–5′ polarity (Hwang et al. 1996; Biswas et al. 2009). StoXPBI destabilized dsDNA with a 3′ extension less efficiently than blunt-ended dsDNA (Fig. 5c). Thus, we demonstrate that dsDNA separation ability of StoXPBI is, in fact, a helix-destabilization activity as the melting activity of SSB (Cubeddu and

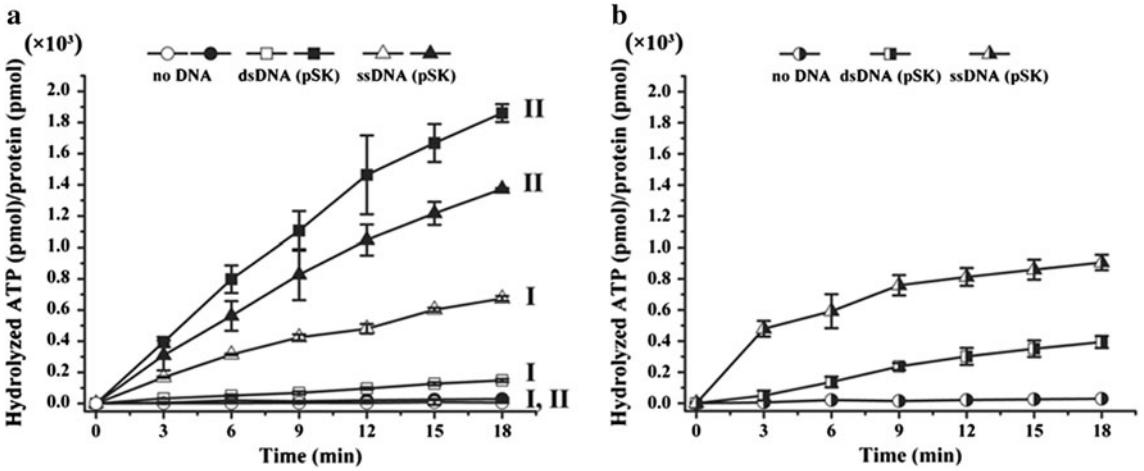

Fig. 3 StoXPBI and StoXPBII are DNA-dependent ATPases. **a** Quantification of the ATPase activity of XPBI and XPBII in the presence or absence of supercoiled double-stranded plasmid DNA and single-stranded virion DNA (pSK, 10 nM). The values are calculated based on three times of independent experiments. *I* XPBI (*open symbols*), *II* XPBII (*filled symbols*), **b** quantification of the ATPase activity of XPBI(112–543) in the presence of supercoiled double-stranded plasmid DNA (*square*) and single-stranded virion DNA (t*riangle* pSK, 10 nM)

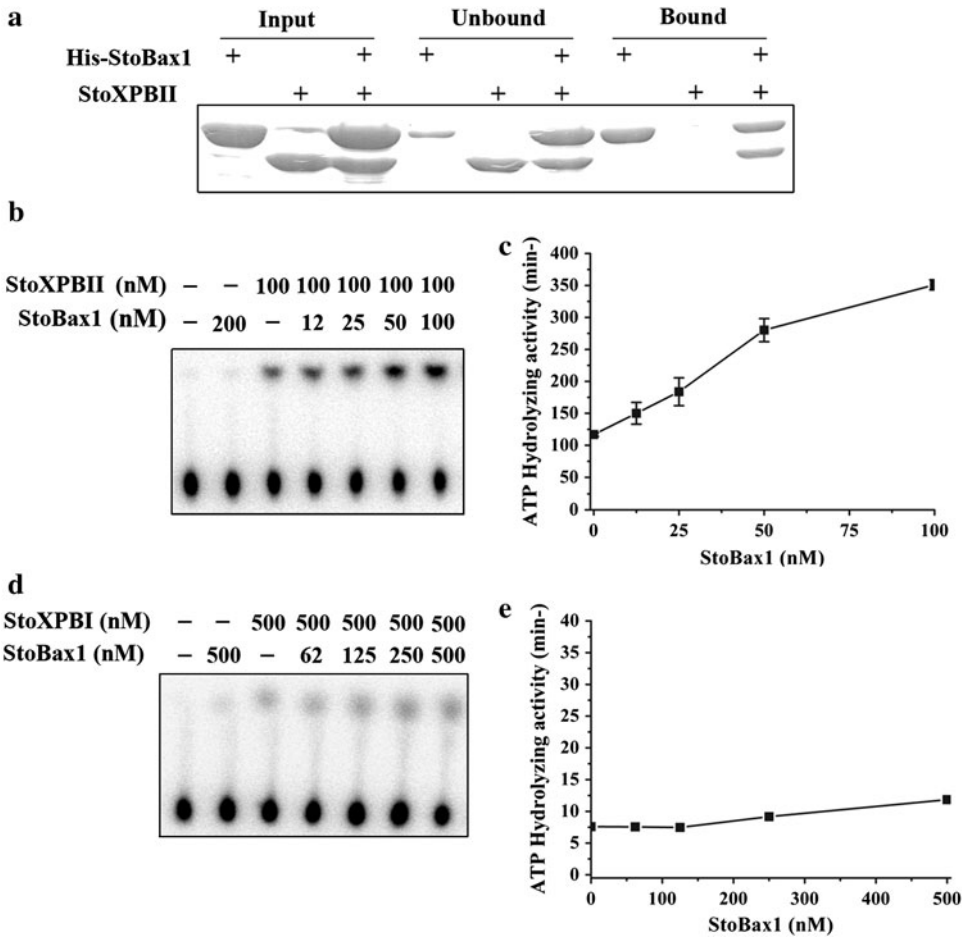

Fig. 4 Analysis of the interaction between XPBII and Bax1. **a** Pull-down assay. Input, the protein fraction mixed with nickel nitrilotriacetic acid-agarose; unbound, the protein fraction unbound to agarose beads; bound, protein fraction bound to agarose beads. **b** A representative gel image showing a stimulation of the ATPase activity of XPBII by Bax1. The assay was performed for 12 min using 3 nM of the supercoiled plasmid, 100 nM XPBII and indicated concentrations of Bax1. **c** Quantification of the results in **b**. **d** A gel image showing that Bax1 is unable to stimulate the ATPase activity of XPBI. The assay was performed for 12 min using 10 nM of the supercoiled plasmid, 500 nM XPBI and indicated concentrations of Bax1. **e** Quantification of the results in **d**. The ATP hydrolyzing activity is calculated as the amount of hydrolyzed ATP (pmol) per enzyme (pmol) per minutes

White 2005), but not a processive helicase activity. To understand if the N-terminal 111 portion of StoXPBI is responsible for the melting activity, we examined the activity of StoXPBI(112–543). As shown in Fig. 6a, the deleted mutant lost the dsDNA melting activity. This result suggests that the N-terminal domain is not only important for

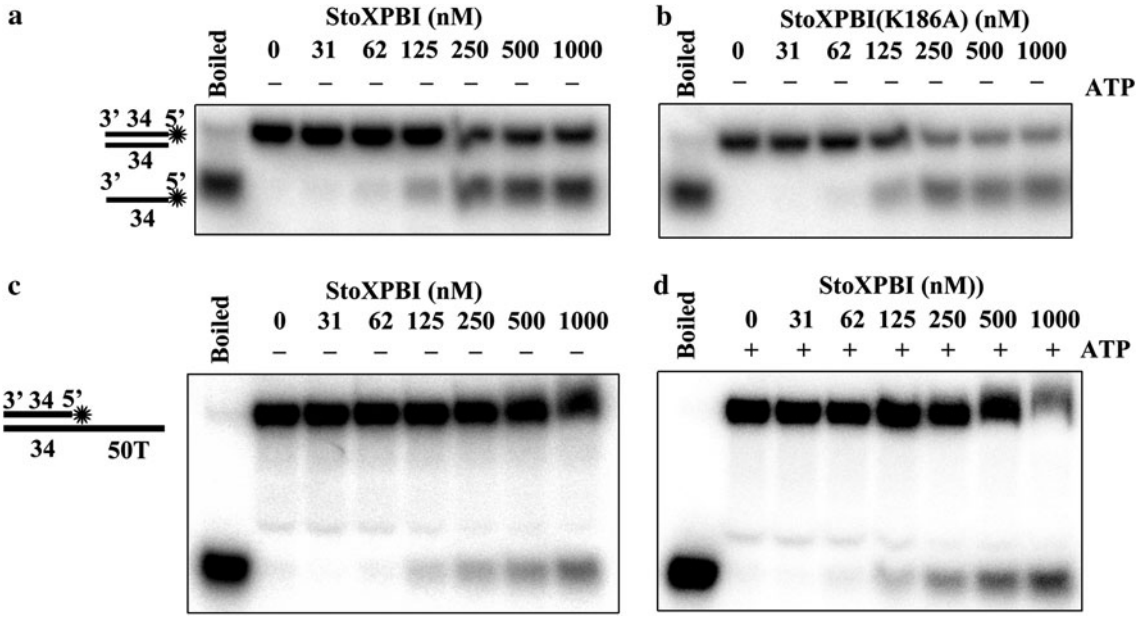

Fig. 5 Analysis of DNA unwinding activity of XPBI. The assays were conducted using blunt-ended dsDNA (**a** and **b**, S1, Table 1) and dsDNA with a 3′ extension (**c** and **d**, S2, Table 1) as the substrates. StoXPBI(K186A) is an ATPase-deficient mutant at the Walk A motif

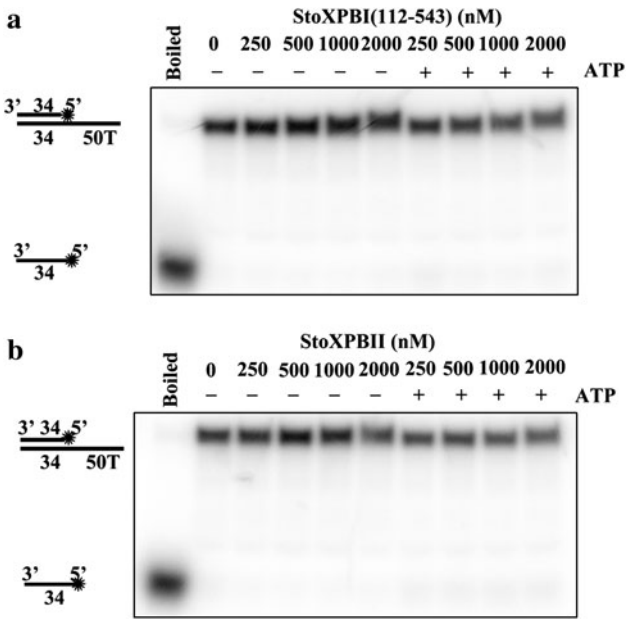

Fig. 6 Assay of DNA unwinding activity of StoXPBI(112–543) and StoXPBII. A dsDNA with a 3′ extension (S2, Table 1) was used as the substrate

the DNA binding of XPBI but also critical for its dsDNA melting activity, and the DNA melting activity may be attributable to its ssDNA binding activity as the melting activity of SSB (Cubeddu and White 2005).

The DNA unwinding activity of StoXPBII was also examined. As shown in Fig. 6b, either in the presence or absence of ATP, StoXPBII did not destabilize the dsDNA substrates under the conditions we used. Neither was StoBax1 able to stimulate the unwinding activity.

The melting activity of StoXPBI is inhibited by ssDNA

It was observed that the dsDNA with a 3′ extension was melted by StoXPBI less efficiently than blunt-ended DNA (Fig. 5a, c). To test the possibility that the ssDNA extension in 3′ overhang substrates inhibits the melting activity, gradient concentrations of ssDNA (A, unlabeled, Table 1) were added into the reactions. Indeed, as the amount of ssDNA increased, the melting activity decreased (Fig. 7a). To further confirm that the melting activity of StoXPBI is inhibited by ssDNA, StoSSB was added into the reaction mixture. SSB could bind the ssDNA extension of substrate and reduce the inhibition caused by ssDNA extension. As expected, although StoSSB itself did not melt dsDNA under the reaction conditions, the melting activity of StoXPBI towards the substrate with 3′ extension increased as increasing amount of StoSSB was added (Fig. 7b). These results suggest that StoXPBI melts DNA depending on its high ssDNA binding activity.

Discussion

NER homologues including XPB helicase are common in eukarya and archaea and studies of the archaeal homologues are expected to obtain important insights into the structure and function of human NER mechanism. Fan

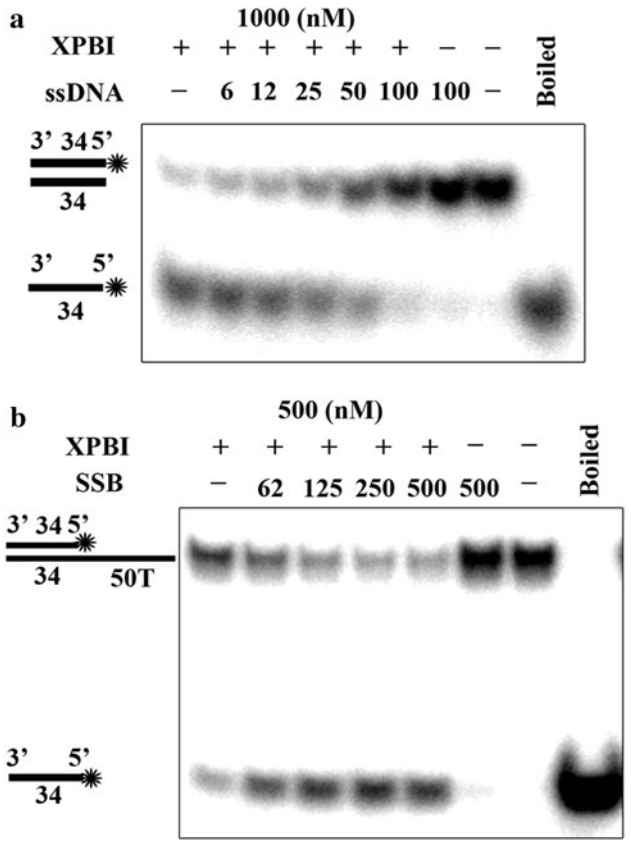

Fig. 7 Inhibition of the melting activity of StoXPBI by ssDNA. **a** A blunt-ended dsDNA substrate was used to test the effect of ssDNA (A, Table 1, 0–100 nM) on the melting activity of StoXPBI (1,000 nM). **b** A substrate dsDNA with a 3′ extension was used to test the effect of SSB (0–500 nM) on the melting activity of StoXPBI (500 nM)

et al. (2006) have reported the structure of XPB homologue from the *Archaeoglobus fulgidus* and show that AfuXPB unwinds dsDNA with a 3′ extension and blunt-ended dsDNA containing a lesion, like CPD or (6–4) photoproducts in vitro. In the crenarchaeon *S. solfataricus*, two XPB homologues, XPBI and XPBII, have been identified and characterized (Richards et al. 2008). Both enzymes are able to bind ssDNA and had DNA-dependent ATPase activity, but neither exhibited helicase activity in vitro under the reported assay conditions.

We analyzed the DNA binding, ATPase, and unwinding activities of XPBI and XPBII from *S. tokodaii*. The DNA binding abilities of StoXPBI and StoXPBII are similar to those of SsoXPBs. The result that StoXPBI and StoXPBII possess DNA-dependent ATPase activity, but do not show processive helicase activity, is also in agreement with that of SsoXPBs (Richards et al. 2008). Interestingly, we show that StoXPBI exhibits an ATP-independent dsDNA destabilization activity in vitro. We detected a similar activity using recombinant XPBI from *S. solfataricus* under our assay conditions at pH from 6.0 to 8.0 (data not shown). Therefore, the ATP-independent activity is perhaps a conserved property of XPBI proteins from both *S. tokodaii* and *S. solfataricus*. In a previous study, no helix destabilization activity of SsoXPBI was observed (Richards et al. 2008). The difference in melting activity between our results and the report in *S. solfataricus* may be due to different reaction temperatures and length of DNA substrates.

It has been reported that, some proteins melt dsDNA, an activity that has important roles in DNA metabolism. For example, the adenovirus DNA-binding protein (DBP) is able to displace oligonucleotides that are annealed to single-stranded M13 DNA independent of ATP and may destabilize duplex DNA ahead of a moving replication fork, thereby assisting in strand displacement during replication (Zijderveld and van der Vliet 1994). SSB from *Sulfolobus* has helix-destabilization activity which is assumed to arise from trapping of transient single-stranded breathing intermediates within DNA duplexes. This activity is proposed to play potential roles in damage recognition (Cubeddu and White 2005). Human RPA is able to melt secondary structures of ssDNA, catalyze strand annealing, and potentially promote Okazaki fragment processing and illegitimate recombination (Bartos et al. 2008).

XPBI may function in creating a substrate for loading of NER proteins at the damage site by the melting activity. It is previously shown that in eukarya the helicase activity of XPB subunit of TFIIH is dispensable for unwinding of damaged DNA and only the helicase activity of XPD subunit is necessary for the damaged DNA unwinding (Coin et al. 2007). XPD monomer cannot unwind damaged DNA efficiently and its efficient unwinding must be activated by interacting proteins in vivo (Pugh et al. 2008). In eukarya, the activity of XPD subunit of the transcription factor IIH (TFIIH) complex is remarkably affected by interaction with p44, another TFIIH component (Coin et al. 2007). However, except XPB and XPD, no homologues of other components of TFIIH in archaea have been identified (reviewed by White 2003). So other factors are needed to promote activity of XPD. XPBI may trap the distorted DNA and melt damaged DNA to form a small bubble and provide XPD with an appropriate substrate. On the other hand, the ATPase activity of XPBI may be used in recruiting proteins to the damaged site or helping the leaving of proteins from DNA.

Our results suggest that the N-terminal domain of XPBI is essential for the ssDNA binding and helix destabilization activity, and is likely involved in forming the suitable substrate. The N-terminal domain is unique and exists in all crenarchaeal XPBIs. Although no conserved motif is found (http://cn.expasy.org/tools/scanprosite/), secondary structure prediction by the JPRED server generates a relatively conserved structure among all crenarchaeal XPBIs

(Supplementary Figure 1). However, the unique N-terminal sequence of XPBI in archaea is different from the N-terminal domain of eukaryotic XPB. The sequence of the N-terminal domain of XPBI is not a homolog of the eukaryotic N-terminal domain which is responsible for the binding of TFIIH to p52 and contains a nuclear localization signal (Jawhari et al. 2002).

It is demonstrated that the endonuclease Bax1 from *Sulfolobus* interacts with XPBII to form a stable complex (Richards et al. 2008) and the *Sulfolobus* Bax1 can cleave DNA at 3′ to the model bubble DNA substrate in complex with XPBII (Rouillon and White 2010), whereas XPB from *T. acidophilum* inhibits the structure-specific nuclease activity of Bax1 (Roth et al. 2009). However, there has been no report about the effect of Bax1 on the activities of XPBII. Here, we demonstrate that StoBax1 can remarkably stimulate the ATPase activity of StoXPBII but has no effect on DNA unwinding. This is reminiscent of p52 subunit of eukaryotic TFIIH. The p52 subunit interacts with XPB and stimulates the ATPase activity of XPB but does not enhance the helicase activity (Coin et al. 2007). Although Bax1 has no sequence similarity with p52, its effect on ATPase activity of XPBII resembles that of p52 (Coin et al. 2007). Like Eukaryotic XPB, it is possible that the ATPase activity of archaeal XPB is mainly not used for providing energy for the helicase action but for recruitment of proteins to the damaged sites of DNA (Oksenych et al. 2009). Bax1 may promote the protein recruitment of XPB through interaction with XPB.

The existence of two XPBs in crenarchaeota raises a question about the roles of the two XPBs in DNA repair. XPBI is more abundant than XPBII in the cells and transcription level of XPBI but not XPBII is up-regulated after UV irradiation (Salerno et al. 2003; Richards et al. 2008). These observations may suggest that XPBI and XPBII have different functions in NER. The difference between XPBI and XPBII in the melting activity and in the ability to interact with Bax1 may support this hypothesis. Rouillon and White (2010) proposed a model that XPBII translocates along the undamaged strand and moves in 3′ to 5′ direction in tandem with XPD, defining the boundary for the 3′ cleavage by Bax1. Based on our results presented in this paper and previous model, we propose that both XPBs are involved in NER. XPBII–Bax1 may translocate along DNA using the energy of ATP hydrolysis and detect the distortion of DNA by the DRD domain of XPBII. Once a lesion is detected, XPBII–Bax1 complex stabilizes itself on DNA by conformational change using the energy of ATP hydrolysis (Oksenych and Coin 2010). XPBI may destabilize the damaged DNA detected by XPBII–Bax1 or other distorted DNA and enlarges the bubble by the DNA melting activity and forms an open intermediate suitable for loading of XPD. After the damaged DNA is unwound by XPD, Bax1 then excises DNA at 3′ to the damaged sites. Analysis using recently established genetic tools may eventually clarify which pathways the two XPBs participate and reveal the role of the ATP-independent melting activity in cellular functions.

Acknowledgments This work was supported by grants from the National Natural Science Foundation of China (30930002 and 30870046 to Y.S., 30770050 to J.N.).

References

Bartos JD, Willmott LJ, Binz SK, Wold MS, Bambara RA (2008) Catalysis of strand annealing by replication protein A derives from its strand melting properties. J Biol Chem 283:21758–21768

Biswas T, Pero J, Joseph C, Tsodikov O (2009) DNA-dependent ATPase activity of bacterial XPB helicases. Biochemistry 48:2839–2848

Coin F, Auriol J, Tapias A, Clivio P, Vermeulen W, Egly JM (2004) Phosphorylation of XPB helicase regulates TFIIH nucleotide excision repair activity. EMBO J 23:4835–4846

Coin F, Oksenych V, Egly JM (2007) Distinct roles for the XPB/p52 and XPD/p44 subcomplexes of TFIIH in damaged DNA opening during nucleotide excision repair. Mol Cell 26:245–256

Cubeddu L, White MF (2005) DNA damage detection by an archaeal single-stranded DNA-binding protein. J Mol Biol 353:507–516

Drapkin R, Reardon JT, Ansari A, Huang JC, Zawel L, Ahn K, Sancar A, Reinberg D (1994) Dual role of TFIIH in DNA excision repair and in transcription by RNA polymerase II. Nature 368:769–772

Fan L, Arvai AS, Cooper PK, Iwai S, Hanaoka F, Tainer JA (2006) Conserved XPB core structure and motifs for DNA unwinding: implications for pathway selection of transcription or excision repair. Mol Cell 22:27–37

Fan L, Fuss JO, Cheng QJ, Arvai AS, Hammel M, Roberts VA, Cooper PK, Tainer JA (2008) XPD helicase structures and activities: insights into the cancer and aging phenotypes from XPD mutations. Cell 133:789–800

Giglia-Mari G, Coin F, Ranish JA, Hoogstraten D, Theil A, Wijgers N, Jaspers NG, Raams A, Argentini M, van der Spek PJ et al (2004) A new tenth subunit of TFIIH is responsible for the DNA repair syndrome trichothiodystrophy group A. Nat Genet 36:714–719

Guzder SN, Sung P, Bailly V, Prakash L, Prakash S (1994) RAD25 is a DNA helicase required for DNA repair and RNA polymerase II transcription. Nature 369:578–581

Hwang JR, Moncollin V, Vermeulen W, Seroz T, van Vuuren H, Hoeijmakers JH, Egly JM (1996) A 3′ to 5′ XPB helicase defect in repair/transcription factor TFIIH of xeroderma pigmentosum group B affects both DNA repair and transcription. J Biol Chem 271:15898–15904

Ishino Y, Nishino T, Morikawa K (2006) Mechanisms of maintaining genetic stability by homologous recombination. Chem Rev 106:324–339

Jawhari A, Lainé JP, Dubaele S, Lamour V, Poterszman A, Coin F, Moras D, Egly JM (2002) P52 mediates XPB function within the transcription/repair factor TFIIH. J Biol Chem 277:31761–31767

Lehmann AR (2008) XPD structure reveals its secrets. DNA Repair (Amst) 7:1912–1915

Lin YC, Choi WS, Gralla JD (2005) TFIIH XPB mutants suggest a unified bacterial-like mechanism for promoter opening but not escape. Nat Struct Mol Biol 12:603–607

Liu H, Rudolf J, Johnson KA, McMahon SA, Oke M, Carter L, McRobbie AM, Brown SE, Naismith JH, White MF (2008) Structure of the DNA repair helicase XPD. Cell 133:801–812

Oh KS, Imoto K, Boyle J, Khan SG, Kraemer KH (2007) Influence of XPB helicase on recruitment and redistribution of nucleotide excision repair proteins at sites of UV-induced DNA damage. DNA Repair (Amst) 6:1359–1370

Oksenych V, Coin F (2010) The long unwinding road: XPB and XPD helicases in damaged DNA opening. Cell Cycle 9:90–96

Oksenych V, de Jesus BB, Zhovmer A, Egly JM, Coin F (2009) Molecular insights into the recruitment of TFIIH to sites of DNA damage. EMBO J 19:2971–2980

Plank JL, Hsieh TS (2006) A novel topologically constrained DNA molecule containing a Double Holliday Junction. J Biol Chem 281:17510–17516

Pugh RA, Lin Y, Eller C, Leesley H, Cann IK, Spies M (2008) *Ferroplasma acidarmanus* RPA2 facilitates efficient unwinding of forked DNA substrates by monomers of FacXPD helicase. J Mol Biol 383:982–998

Richards JD, Cubeddu L, Roberts J, Liu H, White MF (2008) The archaeal XPB protein is a ssDNA-dependent ATPase with a novel partner. J Mol Biol 376:634–644

Roberts JA, White MF (2005a) An archaeal endonuclease displays key properties of both eukaryal XPF-ERCC1 and Mus81. J Biol Chem 280:5924–5928

Roberts JA, White MF (2005b) DNA end-directed and processive nuclease activities of the archaeal XPF enzyme. Nucleic Acids Res 33:6662–6670

Roth HM, Tessmer I, Van Houten B, Kisker C (2009) Bax1 is a novel endonuclease: implications for archaeal nucleotide excision repair. J Biol Chem 284:32272–32278

Rouillon C, White MF (2010) The XPB-Bax1 helicase–nuclease complex unwinds and cleaves DNA: implications for eukaryal and archaeal nucleotide excision repair. J Biol Chem 285: 11013–11022

Rudolf J, Makrantoni V, Ingledew WJ, Stark MJ, White MF (2006) The DNA repair helicases XPD and FancJ have essential iron-sulfur domains. Mol Cell 23:801–808

Salerno V, Napoli A, White MF, Rossi M, Ciaramella M (2003) Transcriptional response to DNA damage in the archaeon *Sulfolobus solfataricus*. Nucleic Acids Res 31:6127–6138

Schaeffer L, Roy R, Humbert S, Moncollin V, Vermeulen W, Hoeijmakers JH, Chambon P, Egly JM (1993) DNA repair helicase: a component of BTF2 (TFIIH) basic transcription factor. Science 260:58–63

Thompson LH, Carrano AV, Sato K, Salazar EP, White BF, Stewart SA, Minkler JL, Siciliano MJ (1987) Identification of nucleotide-excision-repair genes on human chromosomes 2 and 13 by functional complementation in hamster-human hybrids. Somat Cell Mol Genet 13:539–551

Vermeulen W, van Vuuren AJ, Chipoulet M, Schaeffer L, Appeldoorn E, Weeda G, Jaspers NG, Priestley A, Arlett CF, Lehmann AR et al (1994) Three unusual repair deficiencies associated with transcription factor BTF2(TFIIH): evidence for the existence of a transcription syndrome. Cold Spring Harb Symp Quant Biol 59:317–329

White MF (2003) Archaeal DNA repair: paradigms and puzzles. Biochem Soc Trans 31:690–693

Zijderveld DC, van der Vliet PC (1994) Helix-destabilizing properties of the adenovirus DNA-binding protein. J Virol 68:1158–1164